Adsorption Characteristics of 2,4-Dichlorophenoxybutric Acid Using Bamboo Activated Carbon in a Fixed Bed

Tae Young Kim[1,2], Sung Yong Cho[1]

[1]Department of Environmental Energy Engineering, Chonnam National University, Gwangju, Republic of Korea
[2]Department of Environmental Education, Mokpo National University, Jeollanamdo, Republic of Korea
Email: tykim001@jnu.ac.kr

Abstract

Adsorption and desorption characteristics of 2,4-dichlorophenoxybutyric acid (2,4-DB) from aqueous solution on bamboo activated carbon (BAC) were studied in a fixed bed adsorber. The adsorption equilibrium capacity of 2,4-DB on BAC increased with decreasing initial pH of the solution and with a maximum adsorption capacity of 1.61 mol/kg. The adsorption rate of 2,4-DB on BAC could be best fitted by the pseudo first-order model. The adsorption model based on the linear driving force approximation (LDFA) was used for simulating the adsorption behavior of the 2,4-DB in a fixed bed. More than 95% desorption of 2,4-DB was obtained using distilled water.

Keywords

Adsorption, Desorption, 2,4-Dichlorophenoxybutric Acid, Fixed Bed, Kinetic

1. Introduction

Organic pollutants are hazardous compounds that have negative health and environmental effects. Among these organic pollutants, organochlorine compounds are the most common contaminants found in wastewaters and drinking water [1] [2]. Chlorophenoxy derivative such as 2,4-dichlorophenoxyacetic acid, 2,4-dichlorophenoxybutric acid, is a non-biodegradable organic contaminant that has been widely used in pesticides, herbicides, germicides, in the manufacturing of plastics, dyes, antioxidants, paper, and in the petrochemical industries, etc. [3] [4]. Among the numerous agrochemicals in use today, 2,4-dichlorophenoxybutyric acid (2,4-DB), a member of the phenoxy herbicide group, has been widely applied to control broad leaf weeds. 2,4-DB is a selective systemic aux-

in-type herbicide used in agriculture. 2,4-DB causes long-term toxicity when in the water and soil, tissue damage for humans when inhaled, even for a small amount, and harm to the placenta of animals [5] [6] [7]. There are several techniques for removing herbicides from aqueous solution, including ion-exchange [8], reverse osmosis [9], dechlorination [10], ozonation [11], catalytic wet oxidation [12], photocatalytic degradation utilizing TiO₂ [13], solvent extraction [14], ultrasound-assisted magnetic adsorption [15], and adsorption [16]. However, the removal of organic pollutants by activated carbon adsorption is a well-established and broadly used technique for the treatment of domestic and industrial effluents [17] [18] [19]. Activated carbon has typically been employed as an adsorbent for the control of various environmental pollutants, including organics, because of its high pore volume, and large exposed surface area to volume ratio. Although activated carbon has a high adsorption capability for organic contaminants, using commercial activated carbon makes the entire process more expensive [20]. Over the years many researchers have developed low-cost activated carbons utilizing fruit, paper, and textile waste [21]. In this present work, efforts have been undertaken to produce a new and less expensive activated carbon derived from locally available bamboo biomass as source material. Bamboo activated carbon (BAC) impregnated by 50 wt% KOH solution was prepared at 750°C for 1 h and to evaluate the adsorption potential of BAC for 2,4-DB. The surface area and pore size distribution of BAC were obtained by N₂ adsorption and desorption curves. The main purpose of this work is to study the adsorption and desorption characteristics experimentally as well as theoretically to eliminate the 2,4-DB using BAC from aqueous solution. Distilled water was used as desorbate for the 2,4-DB in the economic and environmental point of view.

2. Theoretical Model

Fixed-Bed Adsorption Study

In order to study the adsorption behavior of 2,4-DB in a fixed-bed adsorber, a dynamic model was developed. The adsorption system considered is an isothermal column packed with BAC at a steady state. This model includes the nonlinear adsorption isotherm, the mass balance in the liquid and solid phases, the mass transfer resistance through the adsorbent. The model adopted here utilizes the Langmuir isotherm equation and a linear driving force (LDF) rate model to simplify the diffusional mass transfer inside adsorbent particles. The LDF model is a lumped-parameter model for particle adsorption. A simple model for an isothermal adsorption in a fixed bed is as follows:

Mass balance:

$$-D_L \frac{\partial^2 C_i}{\partial Z^2} + v \frac{\partial C_i}{\partial Z} + \frac{\partial C_i}{\partial t} + \frac{1-\varepsilon_b}{\varepsilon_b} \rho_p \frac{\partial q_i}{\partial t} = 0 \tag{1}$$

where D_L is the axial dispersion coefficient (m²/s), v is the interstitial velocity (m/s), ε_b is the bed voidage, and ρ_p is the particle density (kg/m³).

The boundary conditions are:

$$D_L \left. \frac{\partial C_i}{\partial Z} \right|_{z=0} = -V \left(\left. C_i \right|_{z=0^-} - \left. C_i \right|_{z=0^+} \right) \tag{2}$$

$$\left. \frac{\partial C_i}{\partial Z} \right|_{z=L} = 0 \tag{3}$$

where L and Z are column length (m) and dimensionless bed height, respectively.

The associated initial conditions are:

$$C_i(Z,0) = C_0; \, q_t(Z,0) = 0 \tag{4}$$

The mass-transfer rate inside particles can be represented by

$$\frac{\partial q_i}{\partial t} = k_s \left(q_t^* - q_t \right) \tag{5}$$

where k_s is the effective mass transfer coefficient (m/s), and q_t^* is the equilibrium adsorbed phase concentration.

3. Materials and Methods

3.1. Materials

The biomass adsorbent used in this study was obtained at Damyang (Korea) and cut into particle size in the range of 2 - 3 mm to prepare bamboo chips. In the activation process, the bamboo chips were impregnated by 50 wt% KOH solution for 3 days and then dried at 105°C for 2 days. The obtained biomaterial was placed in a furnace, followed by heating to the carbonization temperature 450°C at an increasing rate of 5°C/min and maintaining at the temperature for 30 min under N_2 atmosphere. Activation temperature 750°C, and maintaining at the temperature for 60 min. Flaked form of BAC was milled using a ball mill and then sieved into a narrow range of particle sizes (0.42 - 0.50 mm). The obtained BAC was washed with deionized water until the pH of neutral. Finally, the BAC was dried in an oven at 105°C for 2 days. All of the reagents, including 2,4-DB (Acros Co. USA), sodium hydroxide and acetic acid were reagent grade.

3.2. Experimental

Adsorption column experiments were carried out in a fixed bed, which was made of a glass column of 2.50 cm in diameter and 50 cm in length. A stainless sieve was attached to the bottom of the column, followed by a layer of glass beads. A known quantity of BAC was packed in the column, to obtain the desired bed height of adsorbent of 10 cm. The column was then filled up with 5 mm size glass beads, in order to provide a uniform flow of the solution through the column. 2,4-DB solution of known concentration, 1.06 mol/m³, was pumped upward through the column at the desired flow rate of 10 - 20 mL/min, controlled by a peristaltic pump. The 2,4-DB solutions at the outlet of the column were collected at regular time intervals for analysis, and the concentrations were

determined using a UV spectrophotometer (Shimadzu 2401PC, Japan) at $\lambda = 284$ nm. The column was lined with a water jacket, and the experiments were performed at 298 K.

4. Results and Discussion

4.1. Adsorption Isotherm and Kinetics

The specific surface area, pore-volume and average pore size of the BAC are measured from N_2 adsorption/desorption isotherm at 77 K (Quantachrome, USA). The specific surface area, pore-volume and average pore size obtained from **Figure 1** were found to be 1664 m^2/g, 0.72 cc/g and 1.74 nm, respectively. As can be seen **Figure 1**, in the low pressure area, the adsorbed amount increases rapidly, which is due to the micro pores filling. Also, there is no distinct hysteresis loop in the high and medium pressure. It indicates that the proportions of meso pores and macro pores are relatively low in BAC.

The adsorption equilibrium amounts of 2,4-DB on BAC was investigated in terms of initial pHs. 1 mol of HCl and NaOH solutions were used to adjust initial pH (3.2, 7, 10) of the solution. The initial pH of the solution is a major factor influencing the adsorption equilibrium capacity of compounds that can be ionized. Acid or alkali species may change the surface chemistry of the adsorbent by reacting with the surface groups, which may lead to significant pH dependent alterations in the adsorption equilibrium. The adsorption equilibrium amounts of 2,4-DB on BAC was evaluated by measuring the adsorption equilibrium data in terms of the initial pH of 2,4-DB solution. The amounts of 2,4-DB adsorbed at equilibrium were calculated from the following mass balance equation:

$$q = \left(C_o - C_e\right)\frac{V}{W}$$ (6)

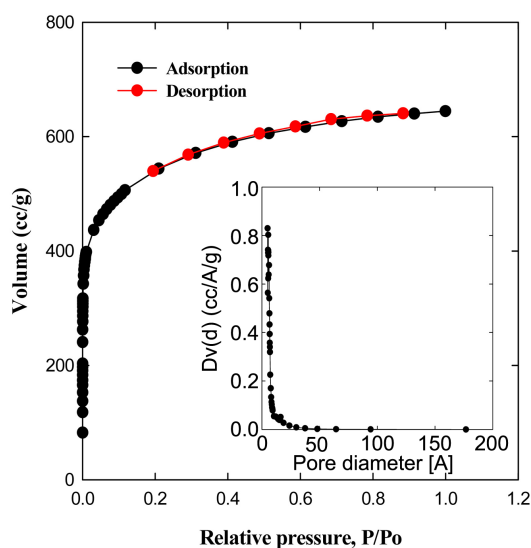where, V is the volume of solution (m^3), and W is the weight of adsorbent (kg).

Figure 1. Adsorption/desorption isotherms of N_2 on BAC and pore size distribution.

Figure 2 shows the adsorption equilibrium isotherm of 2,4-DB on BAC. Adsorption amounts of 2,4-DB on BAC increased with decreasing initial pH of the solution. The similar results were observed in herbicides adsorption on biochars [22] [23] The adsorption equilibrium uptake of 2,4-DB on BAC was 1.61 (pH 3.2), 0.9 (pH 7) and 0.88 mol/kg (pH 10) at 298 K.

The kinetics of 2,4-DB on BAC were analyzed using pseudo-first and pseudo-second order models. The pseudo-first-order rate expression of Lagergren can be expressed as:

$$\frac{\mathrm{d}q}{\mathrm{d}t} = k_1\left(q_{eq} - q_t\right) \tag{7}$$

where, k_1 is the rate constant of first-order adsorption (min^{-1}), and q_{eq} and q_t are the amounts of adsorbed 2,4-DB on BAC at equilibrium, and at time t, respectively. After integration, and applying boundary conditions, $t = 0$ to $t = t$ and $q_t = 0$ to $q_t = q_{eq}$, the integrated form of Equation (7) becomes:

$$\log\left(q_{eq} - q_t\right) = \log q_{eq} - \frac{k_1}{2.303}t \tag{8}$$

A straight line of $\log(q_{eq} - q_t)$ versus t suggests the applicability of this kinetic model (**Figure 3**). If the plot was found to be linear, with a good correlation coefficient, this would indicate that Lagergren's equation is appropriate to 2,4-DB adsorption on BAC. The Lagergren's first-order rate constant (k_1) and $q_{eq,cal}$ determined from the model are presented in **Table 1**, along with the corresponding correlation coefficients. It was seen that the pseudo-first-order model better represented the adsorption kinetics, and the calculated $q_{eq,cal}$ values agreed with the experimental q_{eq} values (**Table 1**). This suggests that the adsorption of 2,4-DB follows first-order kinetics. A similar result was reported for the adsorption of 2,4-D from aqueous solution by granular activated carbon [24].
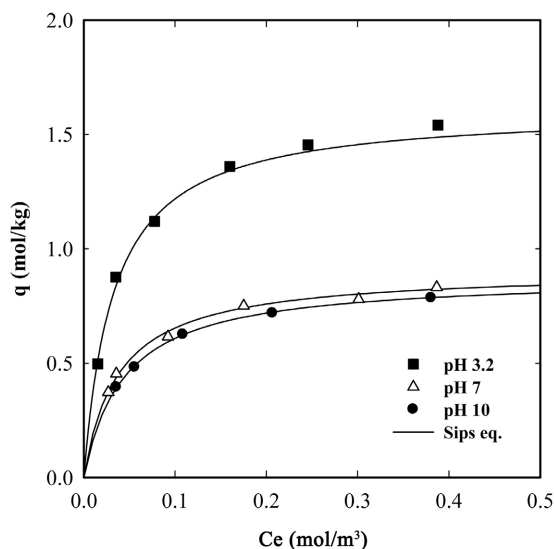

Figure 2. Adsorption equilibrium isotherms of 2,4-DB on BAC in terms of initial pH (298 K).
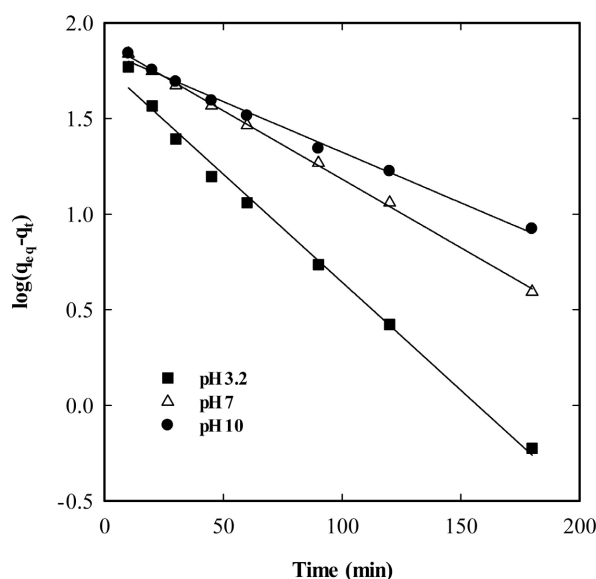
Figure 3. Linearized pseudo-first-order kinetic model in terms of initial pH (298 K).

Table 1. Comparison of the first-order and second-order rate constants obtained at different initial pH (298 K).

		First-order kinetic model			Second-order kinetic model			Measured
		$k_1 \times 10^2$ [min^{-1}]	$q_{eq,cal}$ [mg/g]	R^2	$k_2 \times 10^4$ [g/mg min]	$q_{eq,cal}$ [mg/g]	R^2	$q_{eq,exp}$ [mg/g]
Initial pH	3.2	4.88	101.62	0.99	6.27	111.84	0.99	102.09
	7	2.44	97.05	0.97	3.86	109.63	0.99	99.96
	10	2.31	93.33	0.96	3.67	100.83	0.99	95.95

The pseudo-second-order equation is also based on the sorption capacity of the solid phase, and is expressed as [25]:

$$\frac{dt}{dq} = k_2 \left(q_{eq} - q_t \right)^2 \tag{9}$$

where, k_2 is the rate constant of second-order adsorption (g/mg min). For the same boundary conditions, the integrated form of Equation (9) becomes

$$\frac{t}{q_t} = \frac{1}{k_2 q_{eq}^2} + \frac{1}{q_{eq}} t \tag{10}$$

If second-order kinetics are applicable, the plot of t/q_t against t of Equation (10) should give a linear relationship, from which $q_{eq,cal}$ and k_2, can be determined from the slope and intercept of the plot (**Figure 4**). The k_2 and $q_{eq,cal}$ determined from the model are presented in **Table 1**, along with the corresponding correlation coefficients. It can be seen from **Table 1** that there is no agreement between q_{eq} experimental and q_{eq} calculated values for the pseudo-second-order model.
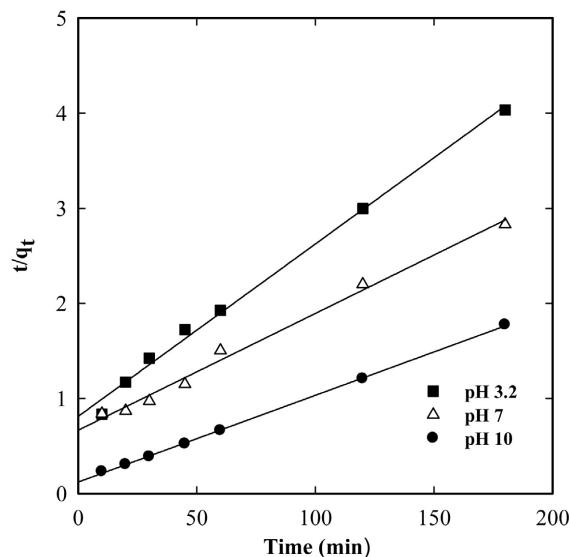
Figure 4. Linearized pseudo-second-order kinetic model in terms of initial pH (298 K).

4.2. Fixed Bed Adsorption

For a packed bed adsorber, the main parameters for mass transfer are the axial dispersion coefficient, and the external film mass transfer coefficient. Axial dispersion contributes to the broadening of the adsorption front axially, due to flow in the interparticle void spaces. Usually it comes from the contribution of molecular diffusion, and the dispersion caused by fluid flow. In this study, the axial dispersion coefficient, D_L, for the fixed bed adsorber was estimated by Wakao's correlation.

$$\frac{D_L}{2vR_p} = \frac{20}{\xi}\left(\frac{D_m}{2vR_p}\right) + \frac{1}{2} = \frac{20}{R_e S_c} + \frac{1}{2} \tag{11}$$

where, ξ is void fraction. External film mass transfer is by diffusion of the adsorbate molecules from the bulk fluid phase, through a stagnant boundary layer surrounding each adsorbent particle, to the external surface of the solid. The external film mass transfer coefficient, k_f, in a fixed bed adsorber can be estimated by the Wakao and Funazkri equation.

$$k_f = \frac{D_m S_h}{2R_p}\left(2.0 + 0.6R_e^{0.5} S_c^{0.33}\right) \tag{12}$$

where, R_e is the Reynolds number defined as $R_e = 2Rv\rho_f / \mu$, S_c is the Schmidt number, $S_c = \mu / D_m \rho_f$ and S_h is the Sherwood number, $S_h = 2k_f R / D_m$, and the molecular diffusion coefficients, D_m, of 2,4-DB can be calculated by the Wilke-Chang equation. The rate of adsorption by porous adsorbents is generally controlled by transport within the particle, rather than by the intrinsic kinetics of sorption at the surface. There are various methods in the literature for determining the diffusion coefficient, here, we determined it by comparing the experimental concentration history in a batch adsorber, with the predicted one based on the pore diffusion model. The estimated values of axial dispersion coefficient, external film mass transfer coefficient, and molecular diffusion are listed in Ta-

ble 2. The breakthrough curves of all species, in general, depend on adsorption equilibrium, intraparticle mass transfer, and the hydrodynamic conditions in the column. Therefore, it is reasonable to consider adsorption equilibrium and mass transport simultaneously, in simulating the adsorption behavior in a fixed bed adsorber. On the other hand, operational factors, such as the initial pH of the solution and flow rate, are important in column design and optimization. In this work, breakthrough curves were obtained under the various experimental conditions mentioned above. In order to demonstrate the effect of the initial pH on the breakthrough curves of 2,4-DB, breakthrough curves under different initial pH values with a constant BAC bed height of 0.075 m, and 2,4-DB initial concentration of 1.06 mol/m³, and flow rate of 6.95 × 10⁻³ m/s are shown in **Figure 5**. The breakthrough time decreased with increase of initial pH value, since the hydrogen ion concentration (pH) has a major effect on the degree of ionization of the sorbate and the surface properties of the adsorbents. These in turn lead to shift in the sorption capacity of the equilibrium sorption process. Since the flow rate is a very important factor in fixed bed design, the effect of flow rate on the adsorption of 2,4-DB on BAC was investigated, by varying the flow rate at 1.02 × 10⁻², 6.95 × 10⁻³ and 3.56 × 10⁻³ m/s, with a constant BAC bed height of 0.075 m, and 2,4-DB initial concentration of 1.06 mol/m³, and initial pH of 3.2. The effect of flow rate on the breakthrough time curves is depicted in **Figure 6**, and shows that the column performed better at a lower flow rate, which resulted in longer breakthrough time and exhaustion times. The breakthrough time decreased with increasing flow rate, and the breakthrough curves are steeper for higher flow rates. This result can be explained by the concept of the moving velocity of the mass transfer zone (MTZ), V_{mtz}, which is defined as follows:

$$V_{mtz} = \frac{\partial z}{\partial t} = \frac{V}{1 + \rho_p \frac{1-\varepsilon_b}{\varepsilon_b}\left(\frac{\partial q}{\partial c}\right)} \tag{13}$$
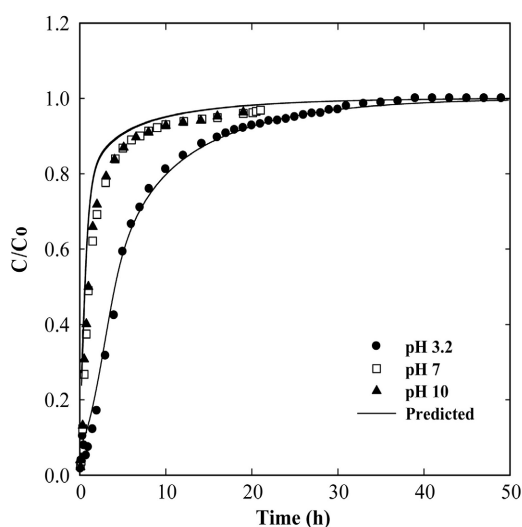

Figure 5. Effects of the initial pH on the experimental results and the model predictions of adsorption breakthrough curves for 2,4-DB on BAC (298 K).
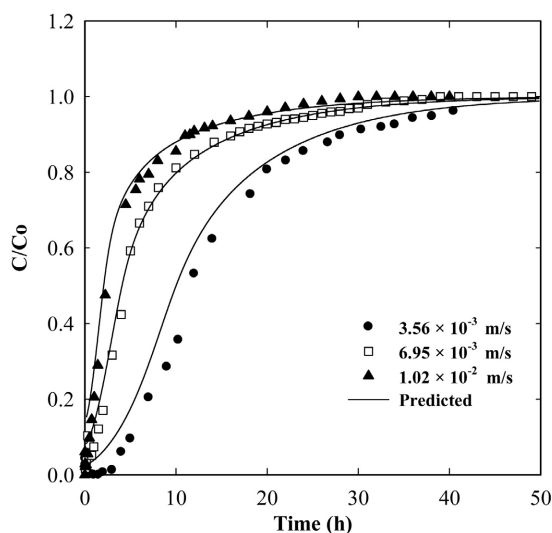
Figure 6. Effects of flow rate on the experimental results and the model predictions of adsorption breakthrough curves for 2,4-DB on BAC (298 K).

Table 2. Model parameters for fixed bed model simulation.

Parameter	Symbol [unit]	Value
Axial dispersion coefficient	D_L [m²/s]	6.19×10^{-6}
Film mass transfer coefficient	k_f [m/s]	6.29×10^{-4}
Molecular diffusion coefficient	D_m [m²/s]	0.139×10^{-9}
Bed porosity	-	0.27

Equation (13) suggests that MTZ is a function of interstitial velocity, particle density, bed porosity, and $\partial q / \partial c$. Intraparticle diffusivity is generally believed to be independent of flow rate. From **Figure 6**, however, the breakthrough curves were found to be steeper at a higher flow rate. This phenomenon is attributed to external film mass transfer resistance. This resistance is smaller when the flow rate is higher, so the length of MTZ is reduced, and a sharp breakthrough curve is generated. In general, the breakthrough curves become steeper, with increasing flow rate and decreasing bed height. Since the intraparticle diffusivity is usually independent of flow rate, this behavior is due to the external film mass transfer resistance. This resistance is weakened when the flow rate is higher, so that the length of the mass transfer zone is reduced, and a sharper breakthrough curve is generated.

For the successful application of an adsorption system, an efficient regeneration of the used adsorbent is very important from the economic point of view. In general, there are many regeneration techniques such as thermal, steam, acid or base and solvent regenerations. The choice of a certain regeneration method should depend upon the physical and chemical characteristics of both the adsorbate and the adsorbent. In this study, distilled water was used as desorbate for the 2,4-DB. As shown in **Figure 7**, desorption of the 2,4-DB in the BAC was
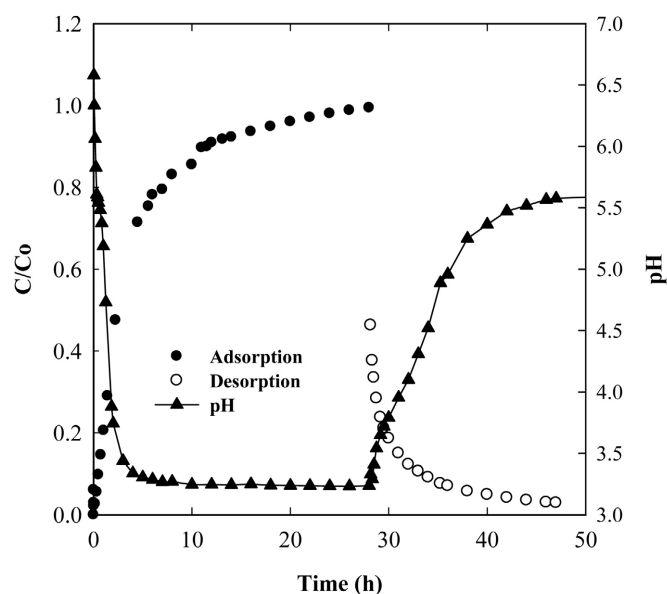
Figure 7. The pH variations during adsorption and desorption processes for the 2,4-DB on BAC (298 K, C_o: 1.06 mol/m³, V_s: 1.02×10^{-2} m/s, H: 0.075 m, initial pH: 3.2).

about 95% using distilled water. The effluent pH increased in the initial stage of adsorption, and decreased to the pH of the initial solution as adsorption proceeded and then increased as desorption proceeded. As discussed previously, the rapid increase of effluent pH in the earlier adsorption stage also implies that large amounts of the 2,4-DB was removed by BAC.

5. Conclusion

The adsorption isotherm capacity of 2,4-DB on BAC increased with decreasing initial pH of the solution. The adsorption equilibrium data was well described by the Sips model. Two simplified models, including pseudo-first-order and pseudo-second-order kinetic models, were used to test the adsorption kinetics. The adsorption rate of 2,4-DB on BAC could be best fitted by the pseudo-first-order model. The breakthrough time of 2,4-DB on BAC decreased with increasing initial pH and flow rate. The proposed simple dynamic model successfully simulated experimental adsorption breakthrough behavior of 2,4-DB under various operating conditions. The desorption yield of the 2,4-DB on BAC was about 95% only using distilled water as solvent.

Acknowledgements

Conflicts of Interest

The authors declare no conflicts of interest regarding the publication of this paper.

References

[1] Ahmaruzzaman, M. (2008) Adsorption of Phenolic Compounds on Low-Cost Adsorbents: A Review. *Advanced in Colloid and Interface Science*, **143**, 48-67. https://doi.org/10.1016/j.cis.2008.07.002

[2] Dąbrowski, A., Podkościelny, P., Hubicki, Z. and Barczak, M. (2005) Adsorption of Phenolic Compounds by Activated Carbon: A Critical Review. *Chemospherem*, **58**, 1049-1070. https://doi.org/10.1016/j.chemosphere.2004.09.067

[3] Sathishkumar, M., Vijayaraghavan, K., Binupriya, A.R., Stephan, A.M., Choi, J.G. and Yun, S.E. (2008) Porogen Effect on Characteristics of Banana Pith Carbon and the Sorption of Dichlorophenols. *Journal of Colloid and Interface Science*, **320**, 22-29. https://doi.org/10.1016/j.jcis.2007.12.011

[4] Zain, N.N.M., Bakar, N.K.A., Mohamad, S. and Saleh, N. (2014) Molecular and Biomolecular Spectroscopy Optimization of a Greener Method for Removal Phenol Species by Cloud Point Extraction and Spectrophotometry. *Spectrochimica Acta Part A*, **118**, 1121-1128. https://doi.org/10.1016/j.saa.2013.09.129

[5] Mazzotta, E. and Malitesta, C. (2010) Electrochemical Detection of the Toxic Organohalide 2,4-DB Using a Co-Porphyrin Based Electrosynthesized Molecularly Imprinted Polymer. *Sensor and Actuators B: Chemical*, **148**, 186-194. https://doi.org/10.1016/j.snb.2010.03.089

[6] Pereiro, I.R., Irimia, R.G., Cano, E.R. and Torrijos, R.C. (2004) Optimization of a Gas Chromatographic-Mass Spectrometric Method for the Determination of Phenoxy Acid Herbicides in Water Samples as Silyl Derivatives. *Analytica Chimica Acta*, **524**, 249-256. https://doi.org/10.1016/j.aca.2004.03.091

[7] Cserhati, T. and Forgacs, E. (1998) Phenoxyacetic Acids: Separation and Quantitative Determination. *Journal of Chromatography B: Biomedical Sciences and Applications*, **717**, 157-178. https://doi.org/10.1016/S0378-4347(98)00028-0

[8] Mourid, E.H., Lakraimi, M. and Legrouri, A. (2022) Preparation of Well-Structured Hybrid Material through Ion Exchange of Chloride by 2,4,5-Trichlorophenoxyacetic Herbicide in a Layered Double Hydroxide. *Materials Chemistry and Physics*, **278**, Article ID: 125570. https://doi.org/10.1016/j.matchemphys.2021.125570

[9] Zhang, J., Weston, G., Yang, X., Gray, S. and Duke, M. (2020) Removal of Herbicide 2-methyl-4-chlorophenoxyacetic Acid (MCPA) from Saline Industrial Wastewater by Reverse Osmosis and Nano Filtration. *Desalination*, **496**, Article ID: 114691. https://doi.org/10.1016/j.desal.2020.114691

[10] Wu, C., Zhou, L., Zhou, Y., Zhou, C., Xia, S. and Rittmann, B.E. (2021) Dechlorination of 2,4-dichlorophenol in a Hydrogen-Based Membrane Palladium-Film Reactor: Performance, Mechanisms, and Model Development. *Water Research*, **188**, Article ID: 116465. https://doi.org/10.1016/j.watres.2020.116465

[11] Contreas, S., Rodriguez, M., Al Momani, F., Sans, C. and Esplugas, S. (2005) Contribution of the Ozonation Pre-Treatment to the Biodegradation of Aqueous Solutions of 2,4-dichlorophenol. *Water Research*, **37**, 3164-3171. https://doi.org/10.1016/S0043-1354(03)00167-2

[12] Oliveira, A.S., Baeza, J.A., De Miera, B.S., Calvo, L., Rodriguez, J.J. and Gilarranz, M.A. (2020) Aqueous Phase Reforming Coupled to Catalytic Wet Air Oxidation for the Removal and Valorisation of Phenolic Compounds in Wastewater. *Journal of Environmental Management*, **274**, Article ID: 111199. https://doi.org/10.1016/j.jenvman.2020.111199

[13] Bayarri, B., Giménez, J., Curcó, D. and Esplugas, S. (2005) Photocatalytic Degradation of 2,4-dichlorophenol by TiO_2/UV: Kinetics, Actinometries and Models. *Catal-*

ysis Today, **101**, 227-236. https://doi.org/10.1016/j.cattod.2005.03.019

[14] Taylor, P., Liu, J., Xie, J., Ren, Z. and Zhang, W. (2013) Treatment Solvent Extraction of Phenol with Cumene from Wastewater. *Desalination and Water Treatment*, **51**, 3826-3831. https://doi.org/10.1080/19443994.2013.796993

[15] Rashtbari, Y., Hazrati, S., Azari, A., Afshin, S., Fazlzadeh, M. and Vosoughi, M. (2020) A Novel, Eco-Friendly and Green Synthesis of PPAC-ZnO and PPAC-nZVI Nanocomposite Using Pomegranate Peel: Cephalexin Adsorption Experiments, Mechanisms, Isotherms and Kinetics. *Advanced Powder Technology*, **31**, 1612-1623. https://doi.org/10.1016/j.apt.2020.02.001

[16] Rubira, R.J.G., Furini, L.N., Constantino, C.J.L. and Sanchez-Cortes, S. (2021) SERS Detection of Prometryn Herbicide Based on Its Optimized Adsorption on Ag Nanoparticles. *Vibrational Spectroscopy*, **114**, Article ID: 103245. https://doi.org/10.1016/j.vibspec.2021.103245

[17] Mahapatra, U., Chatterjee, A., Das, C. and Kumar, A. (2021) Adsorptive Removal of Hexavalent Chromium and Methylene Blue from Simulated Solution by Activated Carbon Synthesized from Natural Rubber Industry Biosludge. *Environmental Technology & Innovation*, **22**, Article ID: 101427. https://doi.org/10.1016/j.eti.2021.101427

[18] Alam, Z., Muyibi, S.A. and Toramae, J. (2007) Statistical Optimization of Adsorption Processes for Removal of 2,4-dichlorophenol by Activated Carbon Derived from oil Palm Empty Fruit Bunches. *Journal of Environmental Sciences*, **19**, 674-677. https://doi.org/10.1016/S1001-0742(07)60113-2

[19] Castro, J.B., Bonelli, P.R., Cerrella, E.G. and Cukierman, A.L. (2000) Phosphoric Acid Activation of Agricultural Residues and Bagasse from Sugar Cane: Influence of the Experimental Conditions on Adsorption Characteristics of Activated Carbons. *Industrial & Engineering Chemistry Research*, **39**, 4166-4172. https://doi.org/10.1021/ie0002677

[20] Bhomick, P.C., Supong, A., Baruah, M. and Pongener, C. (2018) Pine Cone Biomass as an Efficient Precursor for the Synthesis of Activated Biocarbon for Adsorption of Anionic Dye from Aqueous Solution: Isotherm, Kinetic, Thermodynamic and Regeneration Studies. *Sustainable Chemistry and Pharmacy*, **10**, 41-49. https://doi.org/10.1016/j.scp.2018.09.001

[21] Mustafa, R. and Asmatulu, E. (2020) Preparation of Activated Carbon Using Fruit, Paper and Clothing Wastes for Wastewater Treatment. *Journal of Water Process Engineering*, **35**, Article ID: 101239. https://doi.org/10.1016/j.jwpe.2020.101239

[22] Peng, P., Lang, Y.H. and Wang, X.M. (2016) Adsorption Behavior and Mechanism of Pentachlorophenol on Reed Biochars: pH Effect, Pyrolysis Temperature, Hydrochloric Acid Treatment and Isotherms. *Ecological Engineering*, **90**, 225-233. https://doi.org/10.1016/j.ecoleng.2016.01.039

[23] Cabrera, A., Cox, L., Spokas, K., Hermosín, M.C., Cornejo, J. and Koskinen, W.C. (2014) Influence of Biochar Amendments on the Sorption-Desorption of Amino Cyclopy-Rachlor, Bentazone and Pyraclostrobin Pesticides to an Agricultural Soil. *Science of the Total Environment*, **470**-**471**, 438-443. https://doi.org/10.1016/j.scitotenv.2013.09.080

[24] Aksu, Z. and Kabasakal, E. (2004) Batch Adsorption of 2,4-dichlorophenoxyacetic Acid from Aqueous Solution by Granular Activated Carbon. *Separation and Purification Technology*, **35**, 223-240. https://doi.org/10.1016/S1383-5866(03)00144-8

[25] Ho, Y.S. and McKay, G. (1998) Kinetic Models for the Sorption of Dye from Aqueous Solution by Wood. *Process Safety Environment Protection*, **76**, 183-191. https://doi.org/10.1205/095758298529326